Interallelic complementation provides functional evidence for cohesin–cohesin interactions on DNA

Thomas Eng, Vincent Guacci, and Douglas Koshland
Department of Molecular and Cell Biology, University of California, Berkeley, Berkeley, CA 94720

ABSTRACT **The cohesin complex (Mcd1p, Smc1p, Smc3p, and Scc3p) has multiple roles in chromosome architecture, such as promoting sister chromatid cohesion, chromosome condensation, DNA repair, and transcriptional regulation. The prevailing embrace model for sister chromatid cohesion posits that a single cohesin complex entraps both sister chromatids. We report interallelic complementation between pairs of nonfunctional *mcd1* alleles (*mcd1-1* and *mcd1-Q266*) or *smc3* alleles (*smc3-42* and *smc3-K113R*). Cells bearing individual *mcd1* or *smc3* mutant alleles are inviable and defective for both sister chromatid cohesion and condensation. However, cells coexpressing two defective *mcd1* or two defective *smc3* alleles are viable and have cohesion and condensation. Because cohesin contains only a single copy of Smc3p or Mcd1p, these examples of interallelic complementation must result from interplay or communication between the two defective cohesin complexes, each harboring one of the mutant allele products. Neither mcd1-1p nor smc3-42p is bound to chromosomes when expressed individually at its restrictive temperature. However, their chromosome binding is restored when they are coexpressed with their chromosome-bound interallelic complementing partner. Our results support a mechanism by which multiple cohesin complexes interact on DNA to mediate cohesion and condensation.**

Monitoring Editor
Kerry S. Bloom
University of North Carolina

Received: Jun 3, 2015
Revised: Sep 3, 2015
Accepted: Sep 9, 2015

INTRODUCTION

The protein complex cohesin has long been appreciated for its essential role in mediating chromosome architecture (reviewed in Onn *et al.*, 2008). Cohesin is composed of four core subunits: structural maintenance of chromosomes (SMC) Smc1p, Smc3p, Mcd1p/Rad21p/Scc1p, and Scc3p/Irr1p/SAp (Losada *et al.*, 1998). This large protein complex physically links sister chromatids to generate cohesion (Guacci *et al.*, 1997; Michaelis *et al.*, 1997). This cohesion enables each chromosome to achieve bipolar attachment to the spindle, which is critical for promoting high-fidelity segregation of sister chromatids at anaphase. Additional studies revealed that this same complex also plays a role in generating chromosome condensation, regulation of gene expression, and DNA repair (Guacci *et al.*, 1997; Donze *et al.*, 1999; Rollins *et al.*, 1999; Ström *et al.*, 2004; Unal *et al.*, 2004; Yeh *et al.*, 2008; Stephens *et al.*, 2013). These different functions are believed be mediated by cohesin's ability to tether DNA, but using distinct target sites. Cohesion and DNA repair entail tethering two different DNA molecules (intermolecular), whereas condensation and gene regulation tether two different regions of a single DNA molecule (intramolecular) (Guacci *et al.*, 1997; Hartman *et al.*, 2000; Rollins *et al.*, 2004; Ström *et al.*, 2004). Despite cohesin's importance in chromosome architecture, the mechanism by which it generates intramolecular and intermolecular tethers remains an enigma.

The simplest model for chromosome tethering by cohesin is the "embrace" model, which is based on the ring-like or rod-like structure of cohesin that can be visualized in electron micrographs, as well as on a number of biochemical and genetic analyses (Melby *et al.*, 1998; Gruber *et al.*, 2003; Huis In 't Veld *et al.*, 2014). In this model, a single cohesin ring entraps two sister chromatids, thereby tethering them together. For example, during DNA replication, the entrapment of sister chromatids by a cohesin "ring" generates sister chromatid cohesion (Uhlmann and Nasmyth, 1998; Gruber *et al.*, 2003). Alternative models posit that interactions between multiple cohesin complexes (cohesin–cohesin interactions) are required for

This article was published online ahead of print in MBoC in Press (http://www.molbiolcell.org/cgi/doi/10.1091/mbc.E15-06-0331) on September 16, 2015.
Address correspondence to: Douglas Koshland (koshland@berkeley.edu).
Abbreviations used: HA, hemagglutinin; Nz, nocodazole.

cohesion (Guacci *et al.*, 1997; reviewed in Onn *et al.*, 2008; Zhang *et al.*, 2008b). For example, individual cohesin molecules bind a single sister chromatid, and, in turn, dimerization of two DNA-bound cohesins tethers two sister chromatids. It has been of great interest to distinguish between these models and elucidate cohesin's basic mode of action. One way to distinguish between these two models would be to visualize the structure of cohesin as it tethers DNA using high-resolution electron microscopy. Unfortunately, structural approaches like this have not yet been successful.

A cohesin-complex molecule contains a single copy of each of its four subunits (Losada *et al.*, 1998; Tóth *et al.*, 1999; Sumara *et al.*, 2000; Ding *et al.*, 2006; Holzmann *et al.*, 2011). This simple stoichiometry should enable a straightforward biochemical assay to assess whether there are stable interactions between two or more cohesins. This assay entails coexpressing in cells differentially tagged copies of the same cohesin subunit, such as Smc1-3HA and Smc1-MYC, then assessing whether the differentially tagged subunits coimmunoprecipitate. Indeed, such experiments have been conducted in budding yeast and higher eukaryotes (Haering *et al.*, 2002; Gruber *et al.*, 2003; Hauf *et al.*, 2005); one group detected an interaction, but the amounts were low and no biological relevance was shown (Zhang *et al.*, 2008b). One caveat to these studies is that they analyzed solubilized cohesin from cell lysates, whereas putative cohesin–cohesin interactions could be restricted to DNA-bound cohesin. Although it is possible to solubilize chromatin by shearing, coimmunoprecipitation of differentially marked cohesins in the presence of DNA is difficult to interpret. Coimmunoprecipitation could result from a direct interaction between cohesin subunits or an indirect interaction from cohesin subunits bound independently to the same strand of DNA. The lack of robust biochemical or electron microscopic data for dimers or oligomers has led many to favor the idea that cohesin complexes function independently of one another.

A classic genetic signature of protein–protein interaction is often interallelic complementation, such as described for glutamate dehydrogenase, β-galactosidase, ATP-PRTase/His1, or assembly of the Rad52 heptameric ring (Perrin, 1963; Coddington and Fincham, 1965; Korch and Snow, 1973; Reha-Krantz, 1990; Boundy-Mills and Livingston, 1993). In these examples, the products of two mutant alleles in the same gene are defective for function when expressed individually in cells. However, when they are coexpressed in the same cell, they physically interact. The physical interaction restores function. Here we describe the existence of interallelic complementation between either two mutant *mcd1* alleles or two mutant *smc3* alleles. On their own, each mutant *mcd1* or *smc3* allele is inviable and defective for both sister chromatid cohesion and condensation. However, yeast cells coexpressing two defective *mcd1* alleles or two defective *smc3* alleles show robust restoration of viability, cohesion, and condensation. Furthermore, in both cases, the mutant protein of one allele changes the physical properties of the mutant protein from the second allele. These results are consistent with a mechanism by which two or more cohesin complexes directly interact to perform their functions.

RESULTS

Identification of interallelic complementation pairs in recessive cohesin alleles

The *mcd1-Q266* allele of the cohesin's regulatory subunit Mcd1p contains an in-frame, 5–amino acid insertion immediately following residue Q266 (Eng *et al.*, 2014). This allele does not support viability when present as the sole copy of this gene in yeast (Figure 1A; Eng *et al.*, 2014). To study the effect of this lethal allele on cohesion and condensation, we previously introduced this allele into a strain harboring the *MCD1-AID* allele. Proteins fused to auxin-induced degron (AID) undergo ubiquitin-dependent degradation in the presence of the plant hormone auxin (Gray *et al.*, 2001; Nishimura *et al.*, 2009). When *mcd1-Q266 MCD1-AID* cells were treated with auxin, Mcd1-AIDp was degraded, revealing the phenotype of cells harboring only mcd1-Q266p. These cells were inviable as expected and defective in the maintenance of cohesion and the establishment of condensation (Eng *et al.*, 2014).

An alternative and common strategy to study lethal cohesin subunit alleles like *mcd1-Q266* has been to characterize them in strains bearing conditional temperature-sensitive alleles. Indeed for *MCD1*, we and others have used *mcd1-1*, a well-characterized temperature-sensitive allele of *MCD1*, which contains a serine-to-asparagine point mutation at residue 525 (termed *mcd1-1*; Guacci *et al.*, 1997). Few if any cells in a *mcd1-1* culture are viable at the nonpermissive temperature (Figure 1A; Guacci *et al.* 1997). To our surprise, the *mcd1-1 mcd1-Q266* double mutant, containing *mcd1-1* at the endogenous locus and *mcd1-Q266* on a centromere plasmid, is viable at the nonpermissive temperature (Figure 1A). This full restoration of viability argues either for robust interallelic complementation between the *mcd1* alleles or conversion of one of the two alleles to wild-type *MCD1*. We used PCR sequencing to confirm that the double mutant still contained both the *mcd1-1* and *mcd1-Q266* alleles in distinct copies. We also observed robust growth at the nonpermissive temperature in *mcd1-1 mcd1-Q266* strains generated by integrating *mcd1-Q266* at the *URA3* locus of an *mcd1-1* haploid and confirmed the presence of the insertion in *MCD1* by PCR and diagnostic digest (Supplemental Figure S1, A and B). Importantly, when we grew double-mutant cells on 5-fluoroorotic acid (5-FOA) to select for cells that had lost *mcd1-Q266* integrated at the *URA3* locus, the 5-FOA–resistant cells became temperature sensitive (Supplemental Figure S1C). These results confirm that the double mutants still had the *mcd1-1* allele. We also demonstrated allele specificity for complementation, as the lethal *mcd1-V137K* or *mcd1-R135* alleles (Chan *et al.*, 2013; Eng *et al.*, 2014) failed to grow in the *mcd1-1* background at the nonpermissive temperature (Supplemental Figure S2A). Thus this restoration of viability is observed only when cells contain both the *mcd1-1* and *mcd1-Q266* alleles in the *trans* configuration and is due to interallelic complementation.

We discovered two additional examples of interallelic complementation involving a different cohesin subunit, *SMC3*, through our study of the lethal *smc3-K113R* allele. This allele alters a key residue in Smc3p whose acetylation is required for the establishment of cohesion (Rolef Ben-Shahar *et al.*, 2008; Unal *et al.*, 2008; Zhang *et al.*, 2008a). *smc3-K113R* is inviable as sole source from 23 through 37°C (Supplemental Figure S2B; Unal *et al.*, 2008). Initial studies of the *smc3-K113R* allele involved placing it in a temperature-sensitive *smc3-42* background and assessing its function at 37°C. We repeated this analysis at lower nonpermissive temperatures for *smc3-42* than previously examined. Surprisingly, we found that the *smc3-K113R smc3-42* double mutant shows robust viability at 34°C (Figure 1B and Supplemental Figure S2C), whereas the *smc3-K113R* alone or the *smc3-42* allele alone cannot support viability as sole source at 34°C (Figure 1B). We sequenced the *smc3-K113R smc3-42* double mutant and confirmed that both alleles were still present, ruling out gene conversion of either allele to wild-type *SMC3*. Counterselection against *smc3-K113R* by FOA selection confirmed linkage between *smc3-K113R* and suppression of the temperature sensitivity of *smc3-42* cells (Supplemental Figure S1D). The complementation between *smc3-K113R* and *smc3-42* is the second example

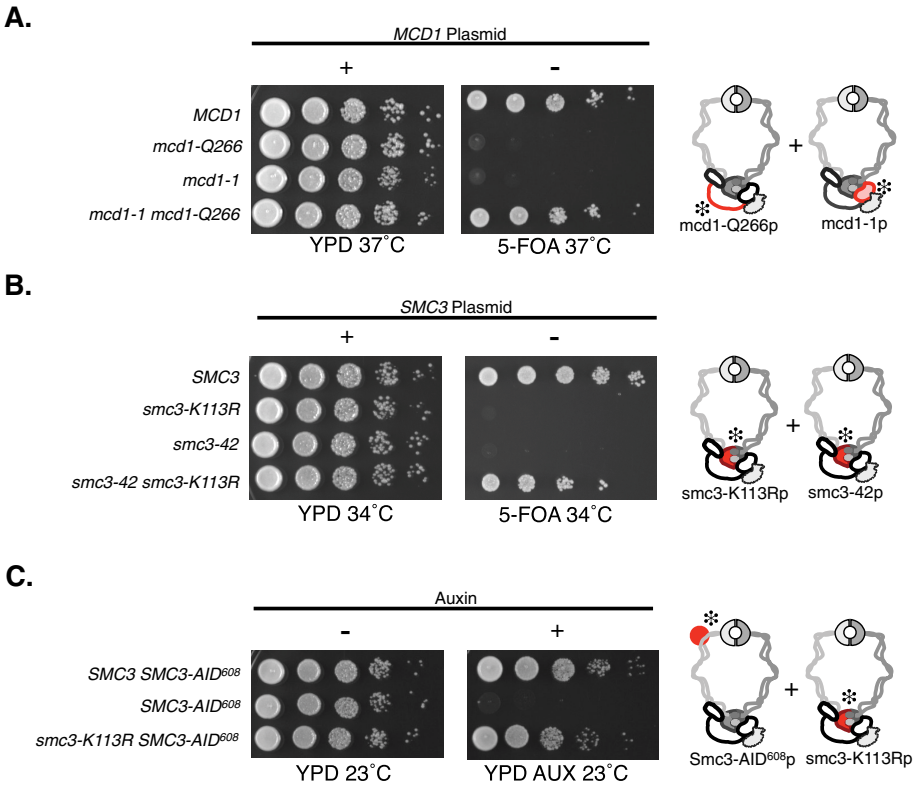

FIGURE 1: Analysis of single- and double-mutant alleles of *mcd1* and *smc3*. (A) All four haploid yeast strains contain an *MCD1* shuffle plasmid pVG201 *{MCD1 URA3 CEN}*. Two strains were deleted for the genomic *MCD1* and contain a second centromere plasmid bearing *MCD1* (*MCD1*; yTE474) or *mcd1-Q266* (*mcd1-Q266*; yTE478). Two strains have the *mcd1-1* allele at the endogenous locus: the parent strain alone (*mcd1-1*; yTE43) or containing a *CEN TRP1* plasmid bearing *mcd1-Q266* (*mcd1-1 mcd1-Q266*; yTE491). Liquid cultures of these four strains were grown to saturation overnight at 23°C and then plated in 10-fold serial dilutions on YPD or 5-FOA and incubated at 37°C for 3 d. Left, relevant *MCD1* genotypes. *MCD1* shuffle plasmid presence (+) or absence (–) is shown above YPD or 5-FOA plates, respectively. Failure to grow on 5-FOA indicates that the *MCD1* shuffle plasmid (pVG201) must be retained. The mutant domains in mcd1-Q266p and mcd1-1p cohesin complexes are highlighted in red and marked with a snowflake. (B) All four haploid yeast strains contain *SMC3* shuffle plasmid pEU42 *{SMC3 URA3 CEN}*. Two strains were deleted for the genomic *SMC3* and contain a second *SMC3* allele at *LEU2* bearing either *SMC3* (*SMC3*; yVG3486-00) or *smc3-K113R* (*smc3-K113R*; yVG3486-K113R). Two strains have the *smc3-42* allele at the endogenous locus: the parent strain alone (*smc3-42*; yTE576) or containing *smc3-K113R* integrated at *LEU2* (*smc3-42 smc3-K113R*; yTE578). Strains were grown and plated as described in A, except that plate incubation was at 34°C. Left, relevant *SMC3* genotypes. *SMC3* shuffle plasmid presence (+) or absence (–) is shown above YPD or 5-FOA plates, respectively. Failure to grow on 5-FOA indicates that pEU42 (wild-type SMC3) must be retained. The mutant domains in smc3-K113Rp and smc3-42p cohesin complexes are highlighted in red and marked with a snowflake. (C) Three haploid yeast strains bear the *SMC3-AID*^{608} at the genomic locus. The parent strain alone (*SMC3-AID*^{608}; yVG3651-3D) or containing a second *SMC3* allele integrated at the *URA3* locus, either wild-type *SMC3* (*SMC3 SMC3-AID*^{608}; yMB81-1A) or *smc3-K113R* (*smc3-K113R SMC3-AID*^{608}; yTE440), were grown at 23°C as described in A. Cells were plated in 10-fold serial dilutions on YPD alone (YPD) or YPD containing 500 µM auxin (YPD AUX) and then incubated for 2 d at 23°C. Left, relevant *SMC3* genotypes. The AID degron near the Smc3 hinge and smc3-K113R cohesin complexes is highlighted in red and marked with a snowflake.

Smc3 protein with an internal auxin degron cassette immediately following residue N607 (Guacci *et al.*, 2015). Strains expressing only the Smc3-AID^{608}p are inviable in the presence of auxin at 23, 30, and 34°C (Figure 1C and Supplemental Figure S2; Guacci *et al.*, 2015). Therefore, to assess *smc3-K113R* function at lower temperatures, we integrated it into the *URA3* locus in an *SMC3-AID*^{608} strain. The *smc3-K113R SMC3-AID*^{608} strain is unable to suppress the auxin-induced lethality at 30 or 34°C (Supplemental Figure S3; unpublished data). However, in the presence of auxin at 23°C, the *smc3-K113R SMC3-AID*^{608} strain grew almost as well as the wild-type *SMC3* strain (Figure 1C). We confirmed that both alleles were still present in the double mutant using PCR sequencing. As a control, we excised the *smc3-K113R* from the *URA3* locus in the double-mutant strain by treatment with 5-FOA (Supplemental Figure S1E). These cells lacking *smc3-K113R* became sensitive to auxin, confirming that suppression of auxin sensitivity requires the *smc3-K113R* allele. Thus *smc3-K113R* complements both the auxin sensitivity of *SMC3-AID*^{608} at 23°C and the temperature sensitivity of *smc3-42* at higher temperatures. The suppression of *SMC3-AID*^{608} and *smc3-42* is allele specific, as the double acetyl-null allele *smc3-K112R, K113R* (*K112/3-RR*) fails to complement the *smc3-42* temperature sensitivity or *SMC3-AID*^{608} on auxin plates (Supplemental Figures S2C and 3B, respectively).

These results demonstrate that three distinct allele pairs of cohesin-complex subunits exhibit interallelic complementation. Of note, the three pairs of complementing alleles occur in multiple regions of the cohesin complex (Figure 1, diagram). The amino acid changes encoded by *mcd1-1*, *mcd1-Q266*, *smc3-42*, and *smc3-K113R* alleles all cluster near cohesin's head domain, although *mcd1-Q266* is located in the linker between the two heads (Figure 1, diagram). However, the *smc3-K113R* and *SMC3-AID*^{608} complementation involves one domain distal to the head, as the AID is in Smc3p's coiled coil proximal to the hinge domain (Figure 1, diagram). Thus interallelic complementation can occur between different domains of cohesin.

of interallelic complementation, indicating that this phenomenon is a characteristic of the cohesin complex rather than a special feature of the *MCD1* cohesin subunit.

The interallelic complementation in *smc3-K113R smc3-42* strains prevented our analysis of smc3-K113Rp alone at lower temperatures. To circumvent this technical difficulty, we used a different conditional *SMC3* allele (*SMC3-AID*^{608}), which encodes an

Interallelic complementation likely occurs by providing distinct activities of cohesin

On the basis of our observations of three diverse sets of interallelic complementation involving two cohesin subunits, we envision two mechanisms for complementation. One possibility is that the product of each mutant allele provides an activity that the other is missing. Alternatively, each mutant allele could have allowed assembly

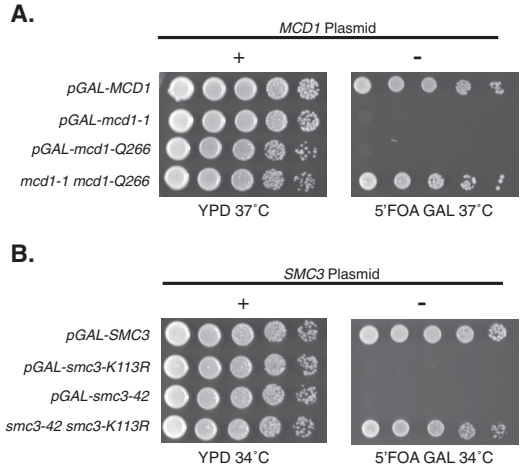

FIGURE 2: GAL1-induced overexpression of *MCD1* and *SMC3* alleles. (A) Four haploid yeast strains contain an *MCD1* shuffle plasmid pVG201 {*MCD1 URA3 CEN*}. Three of these strains are deleted for endogenous *MCD1* and contain a *CEN TRP1* plasmid bearing different *MCD1* alleles under pGAL control: *pGAL-MCD1* (yTE480), *pGAL-mcd1-1* (yTE502), and *pGAL-mcd1-Q266* (yTE482). A positive control has *mcd1-1* at the endogenous locus and *mcd1-Q266* at *LEU2* under their endogenous promoter (*mcd1-1 mcd1-Q266*; TE491). Strains were grown as described in Figure 1A and then plated in 10-fold serial dilutions on YPD or 5-FOA plus galactose (5-FOA GAL) and incubated 3 d at 37°C. *MCD1* shuffle plasmid presence (+) or absence (–) is shown above YPD and 5-FOA GAL, respectively. Failure to grow on 5-FOA GAL indicates that pGAL overexpression alone is insufficient for viability. Left, relevant *MCD1* genotypes. (B) Four haploid yeast strains containing an *SMC3* shuffle plasmid pEU42 {*SMC3 URA3 CEN*}. Three of these strains are deleted for endogenous *SMC3* and contain different *SMC3* alleles under *pGAL* control integrated at *LEU2*: *pGAL-SMC3* (yTE424), *pGAL-smc3-K113R* (yTE449), and *pGAL-smc3-42* (yTE420). A positive control strain has both *smc3-42* and *smc3-K113R* under the endogenous promoter integrated at the *SMC3* and LEU2 loci, respectively (*smc3-42 smc3-K113*; yTE505). Strains were grown as described in Figure 1A and then plated in 10-fold serial dilutions on YPD or 5-FOA plus galactose (5-FOA GAL) and incubated 3 d at 34°C. *SMC3* shuffle plasmid presence (+) or absence (–) is shown above YPD and 5-FOA GAL plates, respectively. Failure to grow on 5-FOA GAL indicates that *pGAL* overexpression alone is insufficient for viability. Left, relevant *SMC3* genotype.

of a complex that was functional but with activity below a level required for viability. When both alleles are present, each contributes the same (reduced) activity, but the sum total of both would meet the threshold required for viability.

If any of the alleles capable of interallelic complementation simply provided cohesin activity below some critical level, then overexpression of the allele might restore cohesin function and viability. To test this possibility, we replaced the endogenous promoter of each mutant allele with the inducible *GAL1* promoter. We then tested the ability of these mutant alleles when overexpressed to support viability as a sole source using the plasmid shuffle strategy. As expected, overexpression of wild-type *MCD1* or *SMC3* using the *GAL1* promoter is viable (Figure 2, A and B, top row). In contrast, *pGAL1*-mediated overexpression of *mcd1-1*, *smc3-K113R*, or *smc3-42* is unable to support viability in the absence of wild type at 34 or 37°C, respectively (Figure 2, A and B, second and third rows). We used Western blots to confirm that mcd1-1 protein levels were dramatically increased after galactose addition (Supplemental Figure S4A). There were no epitope tags on Smc3-K113Rp or smc3-42p, so we used quantitative reverse transcriptase PCR (qRT-PCR) to confirm that the amount of *SMC3*, *smc3-K113R*, and *smc3-42* mRNA dramatically increased after galactose addition (Supplemental Figure S4B). Furthermore, overexpression of these lethal alleles is not sufficient to restore cohesion at the nonpermissive temperature (Supplemental Figure S4C). These results indicate that simply providing more of the product of any single allele (*smc3-42*, *smc3-K113R*, or *mcd1-1*) and its associated activity is insufficient for viability or cohesion. Furthermore, when the same *mcd1* alleles are placed in the *cis* configuration, that is, within the same gene as a "chimeric" *mcd1-1,Q266* allele, it fails to support viability, even when overexpressed (Supplemental Figure S5). Thus the restoration of viability mediated by interallelic complementation likely occurs by each mutant allele providing a distinct activity that is missing in its partner.

Interallelic complementation suppresses the condensation defects characteristic of the single *mcd1* and *smc3* lethal alleles

In budding yeast, cohesin is critical for viability, sister chromatid cohesion, and chromosome condensation. We asked whether the interallelic complementation we observed between pairs of alleles in *MCD1* or *SMC3* for viability reflected complementation of defects in cohesion, condensation, or both. We previously described several examples in budding yeast in which mutants in cohesin or cohesin regulators had little or no cohesion but were viable due to their ability to promote condensation (Guacci and Koshland, 2012). From these results, we concluded that condensation rather than cohesion is the major essential function of cohesin in budding yeast in an unperturbed cell cycle (Guacci and Koshland, 2012). This less-stringent requirement for cohesion compared with other eukaryotes is made possible in budding yeast because of its unusual initiation of spindle assembly during S phase (Guacci and Koshland, 2012; Guacci *et al.*, 2015). This link between cohesin's condensation function and viability led to two predictions regarding interallelic complementation. First, the inviability of each of the single alleles in this study likely reflected a defect in condensation. Second, the viability promoted by interallelic complementation likely reflected their ability to complement each other's defect in condensation.

To test directly these two predictions, we compared condensation in single mutants or in double mutants that exhibited interallelic complementation. For this purpose, cells were synchronized in G1 phase, shifted to conditions nonpermissive for both single alleles, and then released from G1 under nonpermissive conditions and arrested in mid M phase using nocodazole (*Materials and Methods*). Chromosome spreads of these cells in mid M phase were prepared to examine the morphology of the *rDNA* (ribosomal DNA) locus, a well-established metric for condensation in budding yeast (Guacci *et al.*, 1997; Lavoie *et al.*, 2004; Eng *et al.*, 2014). In this assay, proper chromosome condensation results in formation of *rDNA* loops (Figure 3A).

All mutant strains expressing only the single alleles showed a dramatic reduction in *rDNA* loops compared with wild type (Figure 3, B and C, gray bars), consistent with previous results (Guacci *et al.*, 1997; Lavoie *et al.*, 2004; Eng *et al.*, 2014). Thus all single alleles caused a dramatic condensation defect, as expected, given their inviability (Figure 1, A and B, and Supplemental Figure S2). In contrast, both mutant strains expressing allele pairs exhibiting interallelic complementation for viability (*mcd1-1*/*mcd1-Q266* or *smc3-42*/*smc3-K113R* strains) formed *rDNA* loops at levels indistinguishable from

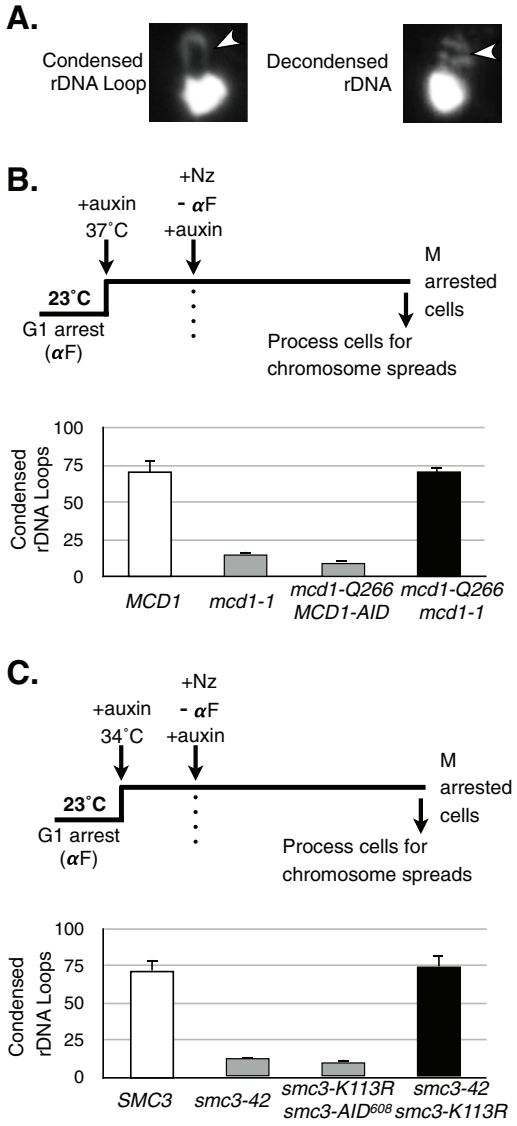

FIGURE 3: Analysis of chromosome condensation in *MCD1* and *SMC3* mutant allele strains. (A) Classification of *rDNA* morphology as assayed by chromosome spreads. Yeast spheroplasts were prepared, and chromosomes were spread on glass slides (see *Materials and Methods*). Chromosome masses were stained using DAPI and scored for morphology of the *rDNA* locus, which is adjacent to the bulk chromosome mass. A loop indicates a condensed *rDNA* locus (left), whereas a puff indicates a decondensed state (right), The *rDNA* is indicated by an arrowhead. (B) Haploid wild-type *MCD1* (yVG3349-1B), *mcd1-1* (yVG3312-7A), *mcd1-Q266 MCD1-AID* (yTE149), and *mcd1-Q266-6MYC mcd1-1* (yTE42) strains were arrested in G1 phase at 23°C, auxin was added to degrade AID-tagged proteins, and shift to 37°C inactivated temperature-sensitive proteins. Cells were released from G1 at 37°C into medium containing auxin and nocodazole to arrest cells in mid M phase. Cells in mid M phase were processed for chromosome spreads and the *rDNA* morphology scored (*Materials and Methods*). The percentage of cells with condensed *rDNA* loops is plotted. At least 200 nuclei were scored for each genotype, and at least two biological replicates were completed for each genotype. (C) Haploid wild-type *SMC3* (yTE45), *smc3-42* (yVG3358-3B), *smc3-K113R smc3-AID^{608}* (yTE440), and *smc3-42 smc3-K113R* (yVG3473-1C) strains were synchronously arrested in mid M phase in auxin-containing medium as described in B, except that the temperature was up-shifted to 34°C. Cells were processed and scored for *rDNA* morphology and the data plotted as the percentage of cells with condensed rDNA loops as described in B. At least 200 DAPI-stained masses were scored for each genotype, and at least two biological replicates were completed for each genotype.

wild type (Figure 3, B and C, compare white and black bars). Thus, as expected, interallelic complementation suppresses both the inviability and condensation defects characteristic of the individual lethal *mcd1* or *smc3* alleles alone.

Interallelic complementation suppresses the cohesion maintenance and establishment defects inherent in the single *mcd1* and *smc3* lethal alleles, respectively

We next asked whether the interallelic complementation that restored both viability and condensation also restores cohesion. We used the regimen described for assaying condensation to obtain cells that progressed from G1 into arrest in mid M phase under conditions in which individual alleles are inactivated. We assayed cohesion in these cells arrested in mid M phase at a centromere-proximal locus (*TRP1*) and at a chromosomal arm locus (*LYS4*), using the LacO/LacI–green fluorescent protein (GFP) system (Straight *et al.*, 1996). In this assay, chromosomes in mid M phase that have cohesion exhibit a single GFP spot, whereas if cohesion is defective, sister separation is detected by the appearance of two GFP spots. A severe cohesion defect is observed in cells expressing only the single-mutant alleles (Figure 4, A and B). In contrast, cells expressing each complementing pair of alleles (*mcd1-1*/*mcd1-Q266* or *smc3-42*/*smc3-K113R*) showed near-wild-type levels of cohesion at both the centromere-proximal and chromosomal arm loci (Figure 4, A and B). Thus the interallelic complementation pairs suppress defects in cohesion, as well as defects in viability and condensation, that are inherent in each lethal *mcd1* or *smc3* allele alone.

Previous studies showed that mutations in cohesin subunits or regulators can lead to defects in either the establishment or maintenance of cohesion (Skibbens *et al.*, 1999; Stead *et al.*, 2003; Noble *et al.*, 2006; Eng *et al.*, 2014). The *mcd1-Q266* allele is defective only in the maintenance of cohesion (Eng *et al.*, 2014), whereas the *mcd1-1* allele is defective in both establishment and maintenance (Guacci *et al.*, 1997; Noble *et al.*, 2006). The robust cohesion observed in *mcd1-1 mcd1*-Q266 cells arrested at mid M phase (Figure 4A) indicates that mcd1-1p and mcd1-Q266p minimally must have complemented their shared defect in cohesion maintenance. It was previously shown that *smc3-42* strains are defective for establishment and maintenance at 35.5 and 37°C (Michaelis *et al.*, 1997; Unal *et al.*, 2008; Guacci and Koshland, 2012). However, *smc3-K113R smc3-42* interallelic complementation is robust at lower temperatures (Figure 1B and Supplemental Figure S2C). Therefore we analyzed cohesion loss at lower temperatures to assess whether, under complementation conditions, defects in cohesion establishment or maintenance are suppressed. The *smc3-42* allele alone had a severe establishment defect, whereas the *smc3-K113R smc3-42* strain established cohesion almost as well as the wild-type strain (Supplemental Figure S6A). The *smc3-K113R smc3-42* strain showed similar restoration of cohesion at 30 and 34°C (Supplemental Figure S6B). Given that condensation is the essential cohesin function, it was formally possible that the *smc3-K113R* allele alone was competent for cohesion, whereas interallelic complementation with the *smc3-42* mutant restored viability and condensation. To rule out this possibility, we needed to assess smc3-K113R under conditions lacking interallelic complementation. Therefore we examined cohesion in an *smc3-K113R smc3-AID^{608}* double mutant at 30 and 34°C, since there is no complementation of viability above 30°C (Supplemental Figure S3A;

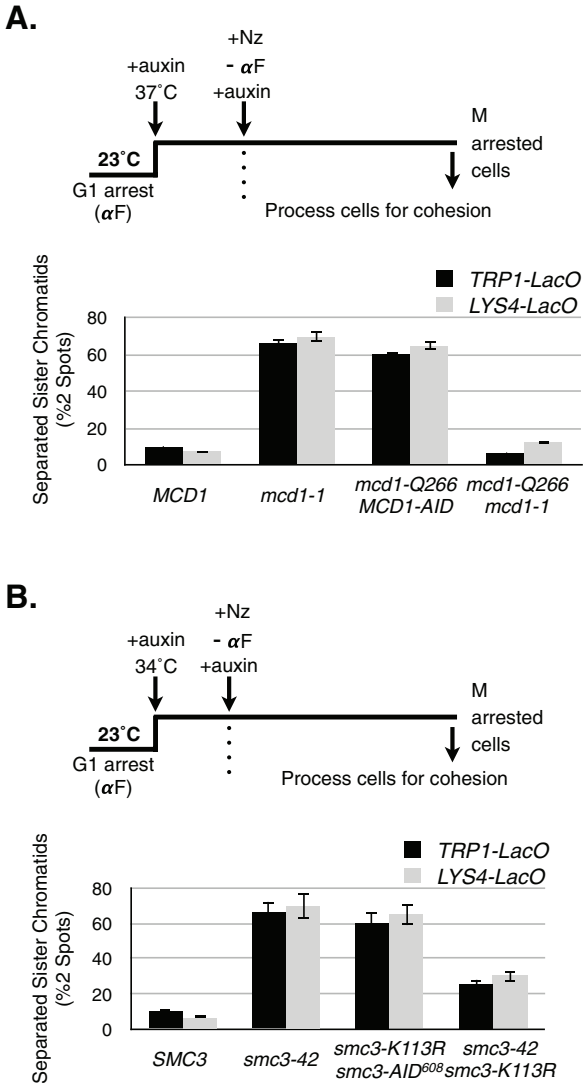

FIGURE 4: Analysis of sister chromatid cohesion at CEN-proximal (*TRP1*) and CEN-distal (*LYS4*) loci in *MCD1* and *SMC3* allele strains. (A) Haploid wild-type *MCD1* (TRP1-LacO: yVG3460-2A and LYS4-LacO: yTE45), *mcd1-1* (TRP1-LacO: yTE453 and LYS4-LacO: yVG3312-7A), *mcd1-Q266 MCD1-AID* (TRP1-LacO: yTE285 and LYS4-LacO: yTE149) and or *mcd1-Q266 mcd1-1* (TRP1-LacO: yTE456 and LYS4-LacO: yTE42) were synchronously arrested in mid M phase at 37°C in medium containing auxin and nocodazole as described in Figure 3B. Cells were processed, fixed, and scored for cohesion at either the *CEN*-proximal *TRP1* locus or the *CEN*-distal *LYS4* locus (*Material and Methods*). The percentage of cells in which sisters had separated (two GFP spots) is plotted. At least 200 cells were scored for each genotype, and the experiment was repeated at least two times to generate data. (B) Haploid wild-type *SMC3* (TRP1-LacO: yVG3460-2A and LYS4-LacO: yTE48), *smc3-42* (TRP1-LacO: yTE494 and LYS4-LacO: yVG3358-3B), *smc3-K113R smc3-AID^{608}* (TRP1-LacO: yTE471 and LYS4-LacO: yTE440), and *smc3-K113R smc3-42* (TRP1-LacO: yTE500 and LYS4-LacO: yVG3473-1C) were synchronously arrested in mid M phase at 34°C in medium containing auxin and nocodazole as described in Figure 3C. Cohesion was scored and plotted as described in A.

unpublished data). In the *smc3-AID^{608}* background, the *smc3-K113R* allele failed to establish cohesion at either 30 or 34°C (Supplemental Figure S6, C and 6). Therefore the robust cohesion in the *smc3-42 smc3-K113R* strain results from interallelic complementation restoring cohesion establishment. Thus interallelic complementation can lead to the restoration of cohesion establishment and maintenance, as well as to condensation and viability.

mcd1-1p is stabilized by the presence of its interallelic complementing partner, mcd1-Q266p

To address the molecular basis underlying these three examples of interallelic complementation, we asked whether the known molecular defects characteristic of each single allele are altered in cells expressing both alleles. A molecular defect of the mcd1-1p is its degradation at 37°C (Figure 5A). We asked whether mcd1-1p degradation is reduced in the presence of its complementing allelic partner, mcd1-Q266p. Cultures of *mcd1-1* and *mcd1-1 mcd1-Q266-6MYC* strains were arrested in mid M phase at 23°C using nocodazole. Each culture was split, and half was incubated at 23°C and half at 37°C for an additional 1 h. Cells were analyzed by Western Blot to assess the mcd1-1p levels using a polyclonal antibody for Mcd1p. As expected for an *mcd1-1* strain, mcd1-1p levels are reduced dramatically after incubation at 37°C compared with 23°C (Figure 5A). In the presence of mcd1-Q266-6MYCp, mcd1-1p levels remained high in cells incubated at 37°C, as seen by the lower–molecular weight band (Figure 5A). The higher–molecular weight band is mcd1-Q266-6MYCp. To rule out the possibility that the lower–molecular weight species detected by our Mcd1p antibody was a degradation product of mcd1-Q266-6MYC, we epitope tagged mcd1-1p with 3xFLAG (mcd1-1-3FLAGp; *Materials and Methods*). We could now unambiguously monitor mcd1-1-3FLAGp via antibodies to its FLAG tag. As expected for the single *mcd1-1-3FLAG* allele strain, anti-FLAG Western blots revealed that the mcd1-1-3FLAGp is degraded at 37°C (Figure 5B). In contrast, in the double-mutant *mcd1-1-3FLAG mcd1-Q266-6MYC* strain, the mcd1-1-3FLAGp is stabilized at 37°C in both S phase– and M phase–arrested cells (Figure 5B). To emphasize, merely increasing mcd1-1p levels by overexpression fails to suppress *mcd1-1* strain inviability or cohesion at 37°C (Figure 2 and Supplemental Figure S4C). Therefore the increased mcd1-1p levels generated by the presence of mcd1-Q266p is not sufficient for viability, but instead the mcd1-Q266p cohesin complex itself is necessary for complementation.

The chromosome-binding defects of mcd1-1p and smc3-AIDp are suppressed by their interallelic complementing partners, mcd1-Q266p and smc3-K113Rp, respectively

mcd1-1p and smc3-42p fail to bind chromosomes at the nonpermissive temperature (Supplemental Figure S7; Haering *et al.*, 2004; Unal *et al.*, 2008), whereas their interallelic partners, mcd1-Q266p and smc3-K113Rp, are bound to chromosomes and cohesin-associated regions (CARs) similar to wild-type cohesin (Rolef Ben-Shahar *et al.*, 2008; Eng *et al.*, 2014). We epitope tagged mcd1-1p (*mcd1-1-3FLAG*) and smc3-42p (*smc3-42-6HA*) to assess whether their binding to chromosomes is restored by the presence of their respective interallelic complementing partners. We first characterized mcd1-1-3FLAG protein in strains bearing the *mcd1-1-3FLAG* allele alone or in the double mutant *mcd1-1-3FLAG mcd1-Q266-6MYC*. Cells were arrested in mid M phase at the nonpermissive temperature (37°C) and processed for global cohesin binding to chromosomes using chromosome spreads and for cohesin binding at CARs and centromere-proximal regions using chromatin immunoprecipitation (ChIP; *Materials and Methods*). As a positive control, we also examined wild-type Mcd1-3FLAGp. For chromosome spreads using anti-FLAG antibodies, as expected, wild-type Mcd1-3FLAGp showed robust chromosomal staining, whereas mcd1-1-3FLAGp

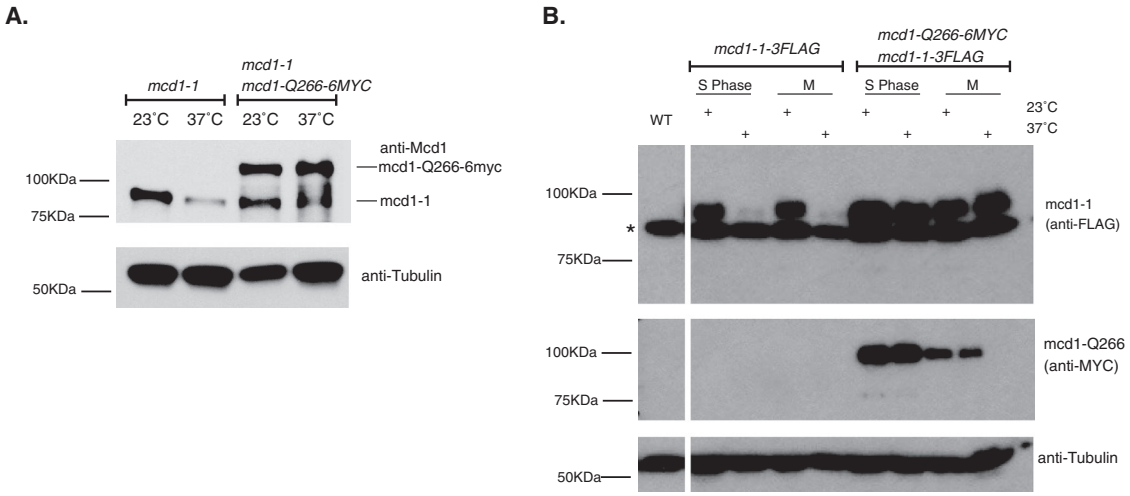

FIGURE 5: Analysis of Mcd1 protein levels in *MCD1* allele strains. (A) Early log phase cultures of haploid strains *mcd1-1* (yVG3312-7A) and *mcd1-1 mcd1-Q266-6MYC* (yTE42) were arrested in M phase with nocodazole for 2.5 h. After all cultures had arrested with 95% large- budded cells, cultures were incubated for an additional 1 h at either 23 or 37°C. Cells were then harvested, lysed, and prepared for protein analysis by SDS–PAGE and Western blotting. Tubulin was used as a loading control. (B) Early log phase cultures of haploid strains *mcd1-1-3FLAG* (yTE103) and *mcd1-1-3FLAG mcd1-Q266-6MYC* (yTE181) were arrested in S phase (hydroxyurea) or M phase (nocodazole) for 2.5 h. After arrest, cultures were split in half and incubated for an additional 1 h at either 23 or 37°C. Afterward, all cultures were harvested, lysed, and prepared for SDS–PAGE and Western blot analysis using mouse anti-FLAG or mouse anti-MYC antibodies to discriminate between both alleles of Mcd1p present. A nonspecific band with a faster mobility than Mcd1-3FLAGp was detected in cells lacking an epitope fusion protein (asterisk). Tubulin was used as a loading control.

did not bind chromosomes (Supplemental Figure S7A). However, when mcd1-Q266-6MYC was present in the same cell, the mcd1-1-3FLAGp bound chromosomes well (Supplemental Figure S7A). We also characterized the smc3-42-6HA protein in strains bearing the *smc3-42-6HA* allele alone or in the double mutant *smc3-K113R smc3-42-6HA* arrested in mid M phase at nonpermissive temperature. Chromosome spreads show that the smc3-42-6HA protein fails to bind chromosomes as the sole source but does bind chromosomes when the complementing *smc3-K113R* allele is also present (Supplemental Figure S7B). Thus the presence of the interallelic complementing partner complements the global chromosomal-binding defects of mcd1-1-3FLAGp and smc3-42-6HAp to a large extent.

ChIP analysis of mcd1-1p and smc3-42p at nonpermissive temperature allowed us to examine this altered binding at higher resolution at CARs on chromosomes I, III, XII, and XIV (*Materials and Methods*; Eng *et al.*, 2014). As expected, wild-type Mcd1-3FLAGp and wild-type Smc3-6HAp show robust binding at CARs and near centromeres (Figure 6, A and B, top), whereas both mutant mcd1-1-3FLAGp and smc3-42-6HAp as sole source have little or no binding (Figure 6, A and B, middle). In contrast, when the complementing alleles are also present in cells, both mcd1-1-3FLAGp and smc3-42-6HAp (Figure 6, A and B, bottom) become enriched at all four regions. Note that this restoration of binding does not reach the levels seen with wild-type proteins. As a control, we show that mcd1-Q266-6MYCp is also bound at all four regions, indicating that it is not displaced by mcd1-1-3FLAGp binding (Supplemental Figure S8). Thus the presence of their interallelic complementing partner dramatically ameliorates the chromosome-binding defects of mcd1-1-3FLAGp and smc3-42-6HAp.

DISCUSSION

Here we provide the first demonstration that cohesin-complex subunits are capable of interallelic complementation. This complementation occurs between specific pairs of nonfunctional *MCD1* alleles, as well as between nonfunctional *SMC3* alleles. Yeast cells expressing only one of these *mcd1* or *smc3* alleles are inviable and defective for both sister chromatid cohesion and condensation. However, cells expressing pairs of these defective *mcd1* or *smc3* alleles become viable and generate cohesion and condensation. Overexpression of any of the individual mutants alone does not restore viability or cohesion, making it unlikely that restoration of viability was a consequence of increasing the activity of one of the two mutant alleles. Furthermore, only certain pairs of alleles are capable of interallelic complementation. Together these observations indicate that interallelic complementation occurs because the individual alleles cause defects in distinct molecular functions of the mutated subunit. It is possible that interallelic complementation had not been previously observed because most mutant alleles abrogate multiple properties of the subunit. The idea that an individual cohesin subunit could have several functional domains is not surprising, given that each subunit interacts with multiple other subunits, and that SMC ATPase regulation entails cross-talk between SMC heads (Hirano, 2001; Haering *et al.*, 2002; Gruber *et al.*, 2003).

The molecular interpretation of our three examples of interallelic complementation is constrained significantly by the known stoichiometry of the cohesin complex. It is well established that each cohesin contains only one copy of each of the subunits (Losada *et al.*, 1998; Tóth *et al.*, 1999; Sumara *et al.*, 2000; Ding *et al.*, 2006; Holzmann *et al.*, 2011). Given this stoichiometry, the interallelic complementation we observe must result from interplay or communication between the two defective cohesin complexes, each harboring one of the mutant allele products. This intercomplex complementation restores a core cohesin activity as it regenerates cohesin's functions in both cohesion and condensation.

One possible mechanism for intercomplex complementation is that one mutant complex indirectly activates the other mutant complex by removing some antagonist to cohesin function. This is

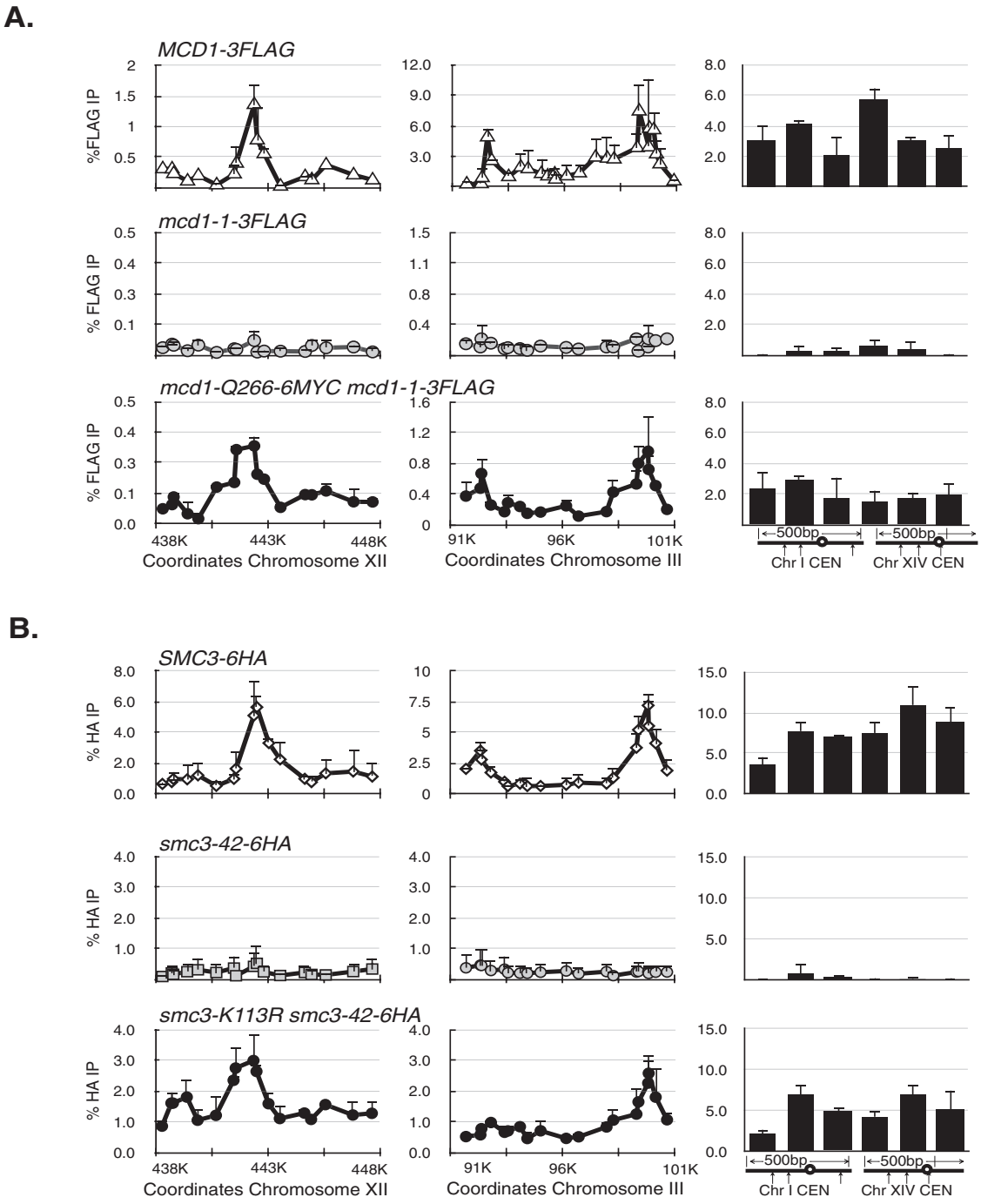

FIGURE 6: Restoration of mcd1-1-3FLAG and smc3-42-6HA binding to chromosomes in interallelic complementation pairs. (A) Haploid *MCD1-3FLAG MCD1-AID* (yTE171), *mcd1-1-3FLAG* (yTE103), and double-mutant *mcd1-1-3FLAG mcd1-Q266-6MYC* (yTE181) strains were grown to early log phase and arrested in mid M phase at 37°C as described in Figure 3B, except that auxin was not added to yTE103 or yTE181. Cells were fixed and processed for chromatin immunoprecipitation using a mouse anti-FLAG antibody (*Materials and Methods*). After immunoprecipitation, CARs (left to right: *CARL1*, *CARC1*, and centromeres I and XIV) were examined by quantitative PCR (qPCR). The percentage of FLAG-tagged Mcd1p immunoprecipitated is plotted vs. total input for all strains (% FLAG IP). The *MCD1* genotype for each strains of interest is indicated above each set of graphs. The average of two biological replicates and the SD between each are shown. (B) Haploid wild-type *SMC3-6HA* (yGC1-8A), *smc3-42-6HA* (yVG3523-1A), and double-mutant *smc3-42-6HA smc3-K113R* (yVG3527-1A) strains were grown to early log phase and then arrested in mid M phase at 34°C as described in Figure 3C, except without auxin addition. Cells were fixed and processed for chromatin immunoprecipitation using a mouse anti-HA antibody (*Materials and Methods*). The same CARs (left to right: *CARL1*, *CARC1*, and centromeres I and XIV) as in A were examined by qPCR. The percentage of HA-tagged Smc3p immunoprecipitated is plotted vs. total input for all strains (% HA IP). The *SMC3* genotype for each strains of interest is indicated above each set of graphs. The average of two biological replicates and the SD between each are shown.

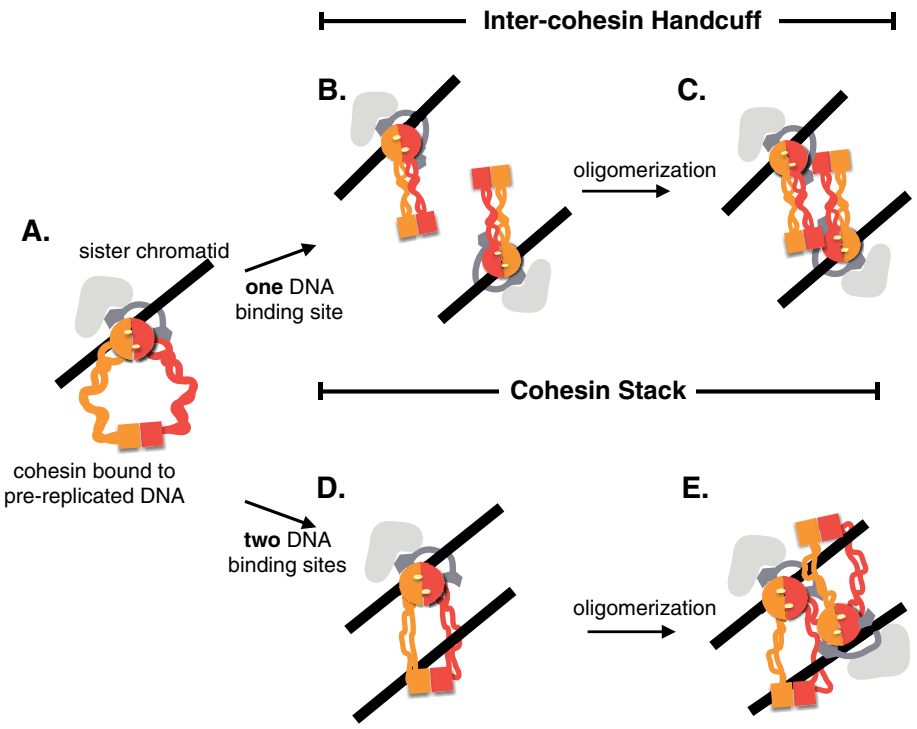

FIGURE 7: Models for cohesin–cohesin interactions as mediators of sister chromatid cohesion. (A) Cohesin is loaded by the Scc2/Scc4 complex onto the unreplicated sister chromatid at the G1/S transition. A topological entrapment of DNA is shown, using the surface formed by the Smc1/Smc3 heads and Mcd1's linker domain. (B, C) Intercohesin handcuff model. (B) Concomitant with DNA replication, a second cohesin complex binds the newly replicated sister chromatid in close proximity to the G1/S-loaded cohesin. Both DNA-bound cohesins undergo a conformational change. (C). Cohesin handcuff state. The conformational change facilitates cohesin oligomerization to tether sister chromatids. Cohesin regulators are likely required to trigger the conformational change (B) and promote/stabilize the oligomeric form (C). (D, E) Cohesin stack model. (D) During DNA replication, the G1/S-loaded cohesin undergoes a conformational change to expose a second cohesin DNA binding motif that holds the sister chromatid. This dual DNA-binding cohesin conformation is not strong enough to tether sisters. (E) This cohesin complex facilitates an oligomerization with adjacent, similarly bound complexes, thus stacking cohesins into a robust tethering form. Cohesin regulators are likely required to promote the conformational change enabling a dual DNA-binding state (D) and to facilitate/stabilize stacking (E).

hard to reconcile with the existing data, as such a putative factor would have to correct several different properties defective in many of the mutant cohesin alleles exhibiting interallelic complementation. For example, *WPL1*, the best-known cohesin inhibitor, cannot be this putative antagonist, as *wpl1Δ* is highly toxic to an *mcd1-1* strain and has no obvious effect on an *smc3-42* strain (Supplemental Figure S9).

Given that in both smc3-42 and mcd1-1 single mutants, the Mcd1p subunit is degraded (this study; Tóth *et al.*, 1999), it could also be that the complementing allele titrates away an Mcd1-specific degradation factor. However, the remarkable suppression of the artificially induced degradation of Smc3-AID^{608}p by smc3-K113R makes this hypothesis also unlikely.

We prefer a model in which the intercomplex complementation is a manifestation of a direct interaction between cohesins on chromosomes that is important for their normal function in cohesion and condensation. Once cohesin has assembled into its core complex, it is competent to bind chromosomes and subsequently undergo cohesin–cohesin interactions. We suggest that smc3-42p and mcd1-1p undergo transient nonproductive binding to chromosomes because cohesins with these mutant subunits are unstable. At nonpermissive temperatures, mcd1-1p is degraded and cohesin binding is lost. In *mcd1-1 mcd1-Q266* cells, the chromosome-bound, mcd1-Q266p–containing cohesin complex interacts with the mcd1-1p containing cohesin complex on DNA (Figures 5 and 6). The same model can apply for the smc3-42p–containing cohesin complexes. Our results with the *SMC3-AID^{608}* complementation suggest that such an interaction must involve multiple subunits in intimate contact. The suppression of the temperature sensitivity of temperature-sensitive proteins through their assembly into larger complexes has many precedents, such as temperature-sensitive virion proteins, which become refractive to temperature inactivation after assembly into the virion (Gordon and King, 1994). By this rationale, cohesin–cohesin interactions could form higher-order structures to facilitate its function in both cohesion and condensation.

Cohesion can be established, but its maintenance can be compromised, without altering cohesin's stable binding to chromosomes (Eng *et al.*, 2014). Other researchers have observed that cohesin at the silent mating locus is stably bound but does not tether sisters (Chang *et al.*, 2005) and that inactivation of cohesin regulators such as Eco1p or Pds5p does not destabilize cohesin's chromosomal binding (Chan *et al.*, 2012, 2013; Guacci and Koshland, 2012; Tong and Skibbens, 2014). This favors a two-step model for cohesin function, as cohesin first stably binds DNA and in turn undergoes a tethering step (Figure 7A). The three types of interallelic complementation pairs we described in this study suggest that an interaction between two or more cohesin molecules (dimerization or oligomerization) is part of this post–DNA binding/tethering activity. Two types of interactions fit these constraints. We call the first model the "intercohesin handcuff" (Figure 7, B and C). Two distinct cohesins could separately bind a sister, and the interaction of these two cohesins could tether the sisters together. In this case, the interaction is essential for cohesin's tethering activity. A second model that fits these constraints is the "cohesin stack" (Figure 7, D and E). Each cohesin molecule would bind both sisters but do so via two distinct DNA-binding sites rather than a single entrapment as postulated by the embrace model. This interaction is insufficient to stably tether sisters (Figure 7D). A second step involving oligomerization of similarly DNA bound cohesins would form an oligomer whose additive DNA binding would be robust enough to tether sisters (Figure 7E). Both of these models are amenable to long-range tethering described for condensation, as well as for gene regulation. Moreover, these new models provide a flexibility by which stably bound cohesin could be repurposed for other chromosome functions by altering oligomerization partners.

If cohesin dimerization or oligomerization is part of the mechanism of cohesin function, why have they not been broadly detected by biochemical methods? Previous biochemical studies examined soluble cohesin complexes and found no robust evidence for cohesin oligomers (Haering *et al.*, 2002; Gruber *et al.*, 2003; Hauf *et al.*, 2005). This failure to observe physical interactions between soluble cohesins is consistent with the idea that such interactions inferred from this study must happen on chromosomes. Interestingly, when cohesin was subjected to a cross-linking reagent in vivo, a number of cross-links between different regions of Smc3p or Smc1p were observed (Huis In 't Veld *et al.*, 2014). These cross-links could represent intramolecular interactions within a subunit. However, in light of our results regarding interallelic complementation, some could represent interactions between two Smc3ps or Smc1ps present in distinct but interacting cohesins. It would be interesting to compare the pattern of cross-links observed with purified soluble cohesin monomers and cohesin bound to chromosomes.

Is this intercomplex interaction a unique property of the cohesin complex, or does it represent a fundamental property conserved in all SMC-family complexes? We strongly suspect that interactions between condensins or other SMC complexes are likely to be important for their function as well. Indeed, a substantial fraction of purified condensin elutes from size exclusion columns at a molecular weight significantly greater than that of a monomeric condensin complex (St-Pierre *et al.*, 2009). This multimeric fraction has robust DNA-supercoiling activity characteristic of condensin, which is more active than the monomeric fraction (Damien D'Amours, personal communication). Miniclusters of condensin complexes have also been observed in reconstituted *Xenopus laevis* chromosomes (König *et al.*, 2007), and condensin may be configured in a "rosette" in the pericentromeric domain (Stephens *et al.*, 2013). Intriguingly, it was recently reported that overexpression of either recessive inviable *SMC4* allele *smc4-7A* or *smc4-82* could restore viability in *smc4-1* cells (Robellet *et al.*, 2015). This result is consistent with interallelic complementation in the condensin complex.

Although the exact molecular basis for cohesin–cohesin interactions revealed in this study remains to be elucidated, their discovery reflects a major molecular component of cohesin function that has escaped previous studies. Their study is likely to provide important new insights into cohesin's molecular and biological functions.

MATERIALS AND METHODS

Yeast strains, media, and reagents

Yeast strains used in this study are in the A364a background, and their genotypes are listed in Supplemental Table S1. Synthetic dropout and yeast extract/peptone/dextrose (YPD) media were prepared as previously described (Guacci *et al.*, 1997). Galactose (2% final [wt/vol]; Sigma-Aldrich, St. Louis, MO) was used as an alternative carbon source to induce genes under the GAL promoter as indicated. For experiments using the AID system, a 1 M stock of 3-indoleacetic acid (auxin; Sigma-Aldrich) dissolved in DMSO was added to plates or liquid cultures at a final concentration of 500 µM, cooling agar used in plates to ~55°C before adding auxin to each batch. The pH of our YPD medium was approximately ~7. To arrest cells in early S phase, we made a 2 M stock solution of hydroxyurea (Sigma-Aldrich), which we added to yeast cells in early log phase to a final concentration of 200 mM. Cell-cycle arrests were visually confirmed when cells were 95% large budded. 5-FOA was purchased from US Biological Life Sciences (Salem, MA) and used at a final concentration of 1 g/l in URA dropout plates supplemented with 50 mg/l uracil powder (Sigma-Aldrich).

Dilution plating assays

Cells were grown to overnight saturation in YPD medium at 23°C (or 30°C when listed), diluted to an OD_{660} of 1.0 using YPD, and then plated in 10-fold serial dilutions. Cells were incubated on different plates at the relevant temperatures indicated.

Shuffle strain construction

SMC3 shuffle strains. Plasmid pEU42 (*SMC3 URA3 CEN*) was transformed into haploid strains. The endogenous *SMC3* gene was deleted and replaced by the HPH cassette (encodes resistance to hygromycin B) using standard PCR-mediated homology-based recombination.

MCD1 shuffle strains. Plasmid *pVG210* (*MCD1 URA3 CEN*) was transformed into haploid strains. The endogenous *MCD1* gene was deleted and replaced by the *KanMx6* cassette.

Shuffle assays. *SMC3* or *MCD1* under their endogenous promoters or under control of the *GAL1* promoter was cloned into *CEN TRP1* plasmids and transformed into *SMC3* or *MCD1* shuffle strains. Alternatively, *SMC3* or *MCD1* alleles were cloned into *LEU2* integrating plasmids, linearized, and then transformed into shuffle stains to integrated constructs at the *LEU2* genomic locus. Transformant clones were grown to saturation in YPD medium at 23°C to allow loss of plasmid pEU42 or pVG210 and then plated in 10-fold serial dilutions on medium containing 5-FOA. 5-FOA selectively kills $URA3^+$ cells, thereby selecting for which of them have lost plasmid pEU42 or pVG210 to become $URA3^-$. This plasmid loss allows assessment of the ability of test alleles on *CEN TRP1* plasmids or integrated at *LEU2* to support viability as the sole *SMC3* or *MCD1* in cells. As a control, cells were also plated on either YPD or URA dropout medium. When test alleles were placed under the *GAL1* promoter, FOA GAL or YP GAL plates were used.

Cell-cycle staging (arrest) in G1 and release into arrest in mid M phase

Haploid yeast strains were grown to mid log phase at 23°C in YPD liquid, and then α factor (Sigma-Aldrich) was added to 10^{-8} M and cells incubated for 3 h to arrest cells in G1 phase. G1-phase arrest was confirmed by presence of unbudded "schmoo" morphology in 95% of the cells as scored by light microscopy and fluorescence-activated cell sorting (FACS). For stains bearing AID-tagged proteins, auxin was added (500 µM final) and cultures incubated 1 h more to induce degradation of AID-tagged proteins. For strains bearing temperature-sensitive alleles, cultures were transferred to the appropriate elevated temperature and then incubated 1 h more to inactivate the temperature-sensitive allele. Cells were released from G1 arrest by six washes in YPD containing 500 µM auxin and 0.1 mg/ml Pronase E (Sigma-Aldrich), resuspended in fresh YPD containing 500 µM auxin and nocodazole (Sigma-Aldrich) at 15 µg/ml final, and then incubated at 23°C for 3 h to allow cell-cycle progression until arrest in mid M phase. Arrest was confirmed by light microscopy for the classical large-budded cellular phenotype (~95% of the population) and by FACS.

Monitoring cohesion using LacO-GFP

Cohesion was monitored using the LacO-LacI system, in which cells contained a GFP-LacI fusion protein and also tandem LacO repeats integrated at one chromosomal locus, which recruits the GFP-LacIp (Straight *et al.*, 1996). *CEN*-distal cohesion was monitored by integrating LacO repeats at *LYS4*, located 470 kb from *CEN4*. *CEN*-proximal cohesion was monitored by integrating LacO

at *TRP1*, located 10 kb from *CEN4*. Cells were fixed and processed to allow the number of GFP signals in each cell to be scored. Before replication, each chromosome exhibits one GFP spot. After replication, chromosomes that have sister chromatid cohesion still exhibit one GFP spot in cells, whereas chromosomes that have lost cohesion exhibit to two GFP spots due to sister separation. The percentage of cells with two GFP spots (separated sisters) was determined and plotted.

Chromosome spreads and microscopy

Chromosome spreads were performed as previously described (Wahba *et al.*, 2013). Slides were incubated with a mouse anti-FLAG monoclonal (Sigma-Aldrich) at 1:4000, mouse anti-V5 (Life Technologies, Carlsbad, CA) at 1:2000, or polyclonal rabbit anti-Mcd1 at 1:4000 dilution. The primary antibody was diluted in blocking buffer (5% bovine serum albumin, 0.2% milk, 1× phosphate-buffered saline, 0.2% Triton X-100). The secondary Cy3-conjugated goat anti-mouse antibody (115-165-003) was obtained from Jackson ImmunoResearch (West Grove, PA) and diluted 1:2000 in blocking buffer. Indirect immunofluorescence was observed using an Olympus IX-70 microscope with a 100×/numerical aperture 1.4 objective and Orca II camera (Hamamatsu, Bridgewater, NJ).

Chromatin immunoprecipitation

Cells used for ChIP experiments were processed as described in Wahba *et al.* (2013). Briefly, after synchronous release from G1 into mitotic arrest, 5×10^8 large-budded cells were fixed for 2 h with 1% formaldehyde. After cell lysis, chromatin was sheared 20 times for 45 s each (settings at duty cycle, 20%; intensity, 10; cycles/burst, 200; 30s of rest between cycles) using a Covaris S2. Immunoprecipitation of epitope-tagged proteins was isolated using anti-FLAG (Sigma-Aldrich), anti-HA (12CA5; Roche Life Sciences, Indianapolis, IN), or anti-MYC (9E10; Roche Life Sciences) monoclonal antibodies. Mcd1p was alternatively immunoprecipitated using a polyclonal rabbit anti-Mcd1 antibody (Covance Biosciences, Princeton, NJ). A no-primary-antibody control was also run to ensure specificity. Appropriate dilutions of input and immunoprecipitated DNA samples were used for quantitative PCR analysis to ensure linearity of the PCR signal. PCR and data analysis was carried out as described previously (Wahba *et al.*, 2013). All experiments were done at least twice, and a representative data set is shown. ChIP primers are available upon request.

Western blotting

Proteins from whole-cell extracts were prepared essentially as described in Foiani *et al.* (1994) with slight modifications. After initial lysis in 300 µl of 20% trichloroacetic acid (TCA; wt/vol), the solution was further diluted with another 300 µl of 5% TCA (wt/vol). The remaining insoluble material was resuspended once more in 500 µl of 5% TCA. These two lysates were combined together and then incubated on ice for 10 min before a 15-min centrifugation at 20,000 × *g* at 4°C. The resulting TCA pellet was resuspended in ~100 µl of loading buffer and pH adjusted with ~10 µl of 1 M Tris, pH 8.0. Resuspended pellets were boiled for 10 min at 70°C, and clarified whole-cell extracts were separated on 7% SDS–PAGE gels under standard laboratory conditions.

Microscopy

Images were acquired with an Axioplan2 microscope (100× objective, numerical aperture 1.40; Zeiss, Thornwood, NY) equipped with a Quantix charge-coupled device camera (Photometrics, Tucson, AZ).

Flow cytometry

DNA content of cells was analyzed using flow cytometry as described previously (Eng, 2014; Guacci *et al.*, 2015).

ACKNOWLEDGMENTS

We thank Anjali Krishnan, Hugo Tapia, Lorenzo Costantino, Gamze Camdere, and Elçin Ünal for helpful discussions, reagents, and constructive feedback on the manuscript. This work was supported by Grant R01 GM092813 from the National Institute of General Medical Sciences/National Institutes of Health to D.E.K. and a National Science Foundation Graduate Research Fellowship to T.E.

REFERENCES

Boundy-Mills KL, Livingston DM (1993). A Saccharomyces cerevisiae RAD52 allele expressing a C-terminal truncation protein: activities and intragenic complementation of missense mutations. Genetics 133, 39–49.

Chan K-L, Gligoris T, Upcher W, Kato Y, Shirahige K, Nasmyth K, Beckouët F (2013). Pds5 promotes and protects cohesin acetylation. Proc Natl Acad Sci USA 110, 13020–13025.

Chan K-L, Roig MB, Hu B, Beckouët F, Metson J, Nasmyth K (2012). Cohesin's DNA exit gate is distinct from its entrance gate and is regulated by acetylation. Cell 150, 961–974.

Chang C-R, Wu C-S, Hom Y, Gartenberg MR (2005). Targeting of cohesin by transcriptionally silent chromatin. Genes Dev 19, 3031–3042.

Coddington A, Fincham JR (1965). Proof of hybrid enzyme formation in a case of inter-allelic complementation in neurospora crassa. J Mol Biol 12, 152–161.

Ding D-Q, Sakurai N, Katou Y, Itoh T, Shirahige K, Haraguchi T, Hiraoka Y (2006). Meiotic cohesins modulate chromosome compaction during meiotic prophase in fission yeast. J Cell Biol 174, 499–508.

Donze D, Adams CR, Rine J, Kamakaka RT (1999). The boundaries of the silenced HMR domain in Saccharomyces cerevisiae. Genes Dev 13, 698–708.

Eng T, Guacci V, Koshland D (2014). ROCC, a conserved region in cohesin's Mcd1 subunit, is essential for the proper regulation of the maintenance of cohesion and establishment of condensation. Mol Biol Cell 25, 2351–2364.

Foiani M, Marini F, Gamba D, Lucchini G, Plevani P (1994). The B subunit of the DNA polymerase alpha-primase complex in Saccharomyces cerevisiae executes an essential function at the initial stage of DNA replication. Mol Cell Biol 14, 923–933.

Gordon CL, King J (1994). Genetic properties of temperature-sensitive folding mutants of the coat protein of phage P22. Genetics 136, 427–438.

Gray WM, Kepinski S, Rouse D, Leyser O, Estelle M (2001). Auxin regulates SCF(TIR1)-dependent degradation of AUX/IAA proteins. Nature 414, 271–276.

Gruber S, Haering CH, Nasmyth K (2003). Chromosomal cohesin forms a ring. Cell 112, 765–777.

Guacci V, Koshland D (2012). Cohesin-independent segregation of sister chromatids in budding yeast. Mol Biol Cell 23, 729–739.

Guacci V, Koshland D, Strunnikov A (1997). A direct link between sister chromatid cohesion and chromosome condensation revealed through the analysis of MCD1 in S. cerevisiae. Cell 91, 47–57.

Guacci V, Stricklin J, Bloom MS, Guō X, Bhatter M, Koshland D (2015). A novel mechanism for the establishment of sister chromatid cohesion by the ECO1 acetyltransferase. Mol Biol Cell 26, 117–133.

Haering CH, Löwe J, Hochwagen A, Nasmyth K (2002). Molecular architecture of SMC proteins and the yeast cohesin complex. Mol Cell 9, 773–788.

Haering CH, Schoffnegger D, Nishino T, Helmhart W, Nasmyth K, Löwe J (2004). Structure and stability of cohesin's Smc1-kleisin interaction. Mol Cell 15, 951–964.

Hartman T, Stead K, Koshland D, Guacci V (2000). Pds5p is an essential chromosomal protein required for both sister chromatid cohesion and condensation in Saccharomyces cerevisiae. J Cell Biol 151, 613–626.

Hauf S, Roitinger E, Koch B, Dittrich CM, Mechtler K, Peters J-M (2005). Dissociation of cohesin from chromosome arms and loss of arm cohesion during early mitosis depends on phosphorylation of SA2. PLoS Biol 3, e69.

Hirano M (2001). Bimodal activation of SMC ATPase by intra- and intermolecular interactions. EMBO J 20, 3238–3250.

Holzmann J, Fuchs J, Pichler P, Peters J-M, Mechtler K (2011). Lesson from the stoichiometry determination of the cohesin complex: a short protease mediated elution increases the recovery from cross-linked antibody-conjugated beads. J Proteome Res 10, 780–789.
Huis In 't Veld PJ, Herzog F, Ladurner R, Davidson IF, Piric S, Kreidl E, Bhaskara V, Aebersold R, Peters J-M (2014). Characterization of a DNA exit gate in the human cohesin ring. Science 346, 968–972.
Korch CT, Snow R (1973). Allelic complementation in the first gene for histidine biosynthesis in Saccharomyces cerevisiae. I. Characteristics of mutants and genetic mapping of alleles. Genetics 74, 287–305.
König P, Braunfeld MB, Sedat JW, Agard DA (2007). The three-dimensional structure of in vitro reconstituted Xenopus laevis chromosomes by EM tomography. Chromosoma 116, 349–372.
Lavoie BD, Hogan E, Koshland D (2004). In vivo requirements for rDNA chromosome condensation reveal two cell-cycle-regulated pathways for mitotic chromosome folding. Genes Dev 18, 76–87.
Losada A, Hirano M, Hirano T (1998). Identification of Xenopus SMC protein complexes required for sister chromatid cohesion. Genes Dev 12, 1986–1997.
Melby TE, Ciampaglio CN, Briscoe G, Erickson HP (1998). The symmetrical structure of structural maintenance of chromosomes (SMC) and MukB proteins: long, antiparallel coiled coils, folded at a flexible hinge. J Cell Biol 142, 1595–1604.
Michaelis C, Ciosk R, Nasmyth K (1997). Cohesins: chromosomal proteins that prevent premature separation of sister chromatids. Cell 91, 35–45.
Nishimura K, Fukagawa T, Takisawa H, Kakimoto T, Kanemaki M (2009). An auxin-based degron system for the rapid depletion of proteins in nonplant cells. Nat Methods 6, 917–922.
Noble D, Kenna MA, Dix M, Skibbens RV, Unal E, Guacci V (2006). Intersection between the regulators of sister chromatid cohesion establishment and maintenance in budding yeast indicates a multi-step mechanism. Cell Cycle 5, 2528–2536.
Onn I, Heidinger-Pauli JM, Guacci V, Unal E, Koshland DE (2008). Sister chromatid cohesion: a simple concept with a complex reality. Annu Rev Cell Dev Biol 24, 105–129.
Perrin D (1963). Immunological studies with genetically altered beta-galactosidases. Ann NY Acad Sci 103, 1058–1066.
Reha-Krantz LJ (1990). Genetic evidence for two protein domains and a potential new activity in bacteriophage T4 DNA polymerase. Genetics 124, 213–220.
Robellet X, Thattikota Y, Wang F, Wee T-L, Pascariu M, Shankar S, Bonneil É, Brown CM, D'Amours D (2015). A high-sensitivity phospho-switch triggered by Cdk1 governs chromosome morphogenesis during cell division. Genes Dev 29, 426–439.
Rolef Ben-Shahar T, Heeger S, Lehane C, East P, Flynn H, Skehel M, Uhlmann F (2008). Eco1-dependent cohesin acetylation during establishment of sister chromatid cohesion. Science 321, 563–566.
Rollins RA, Korom M, Aulner N, Martens A, Dorsett D (2004). Drosophila nipped-B protein supports sister chromatid cohesion and opposes the stromalin/Scc3 cohesion factor to facilitate long-range activation of the cut gene. Mol Cell Biol 24, 3100–3111.
Rollins RA, Morcillo P, Dorsett D (1999). Nipped-B, a Drosophila homologue of chromosomal adherins, participates in activation by remote enhancers in the cut and Ultrabithorax genes. Genetics 152, 577–593.
Skibbens RV, Corson LB, Koshland D, Hieter P (1999). Ctf7p is essential for sister chromatid cohesion and links mitotic chromosome structure to the DNA replication machinery. Genes Dev 13, 307–319.
Stead K, Aguilar C, Hartman T, Drexel M, Meluh P, Guacci V (2003). Pds5p regulates the maintenance of sister chromatid cohesion and is sumoylated to promote the dissolution of cohesion. J Cell Biol 163, 729–741.
Stephens AD, Quammen CW, Chang B, Haase J, Taylor RM, Bloom K (2013). The spatial segregation of pericentric cohesin and condensin in the mitotic spindle. Mol Biol Cell 24, 3909–3919.
St-Pierre J, Douziech M, Bazile F, Pascariu M, Bonneil É, Sauvé V, Ratsima H, D'Amours D (2009). Polo kinase regulates mitotic chromosome condensation by hyperactivation of condensin DNA supercoiling activity. Mol Cell 34, 416–426.
Straight AF, Belmont AS, Robinett CC, Murray AW (1996). GFP tagging of budding yeast chromosomes reveals that protein-protein interactions can mediate sister chromatid cohesion. Curr Biol 6, 1599–1608.
Ström L, Lindroos HB, Shirahige K, Sjögren C (2004). Postreplicative recruitment of cohesin to double-strand breaks is required for DNA repair. Mol Cell 16, 1003–1015.
Sumara I, Vorlaufer E, Gieffers C, Peters BH, Peters JM (2000). Characterization of vertebrate cohesin complexes and their regulation in prophase. J Cell Biol 151, 749–762.
Tong K, Skibbens RV (2014). Cohesin without cohesion: a novel role for Pds5 in Saccharomyces cerevisiae. PLoS One 9, e100470.
Tóth A, Ciosk R, Uhlmann F, Galova M, Schleiffer A, Nasmyth K (1999). Yeast cohesin complex requires a conserved protein, Eco1p(Ctf7), to establish cohesion between sister chromatids during DNA replication. Genes Dev 13, 320–333.
Uhlmann F, Nasmyth K (1998). Cohesion between sister chromatids must be established during DNA replication. Curr Biol 8, 1095–1101.
Unal E, Arbel-Eden A, Sattler U, Shroff R, Lichten M, Haber JE, Koshland D (2004). DNA damage response pathway uses histone modification to assemble a double-strand break-specific cohesin domain. Mol Cell 16, 991–1002.
Unal E, Heidinger-Pauli JM, Kim W, Guacci V, Onn I, Gygi SP, Koshland DE (2008). A molecular determinant for the establishment of sister chromatid cohesion. Science 321, 566–569.
Wahba L, Gore SK, Koshland D (2013). The homologous recombination machinery modulates the formation of RNA-DNA hybrids and associated chromosome instability. Elife 2, e00505.
Yeh E, Haase J, Paliulis LV, Joglekar A, Bond L, Bouck D, Salmon ED, Bloom KS (2008). Pericentric chromatin is organized into an intramolecular loop in mitosis. Curr Biol 18, 81–90.
Zhang J, Shi X, Li Y, Kim BJ, Jia J, Huang Z, Yang T, Fu X, Jung SY, Wang Y, *et al*. (2008a). Acetylation of Smc3 by Eco1 is required for S phase sister chromatid cohesion in both human and yeast. Mol Cell 31, 143–151.
Zhang N, Kuznetsov SG, Sharan SK, Li K, Rao PH, Pati D (2008b). A handcuff model for the cohesin complex. J Cell Biol 183, 1019–1031.